

Structural Identification of a Non-Glycosylated Variant at Ser126 for O-Glycosylation Site from EPO BRP, Human Recombinant Erythropoietin by LC/MS Analysis

Jaehee Byeon¹, Yu-Ri Lim², Hyong-Ha Kim³, and Jung-Keun Suh^{1,4,*}

A variant peak was detected in the analysis of RP-HPLC of rHu-EPO, which has about 7% relative content. Fractions of the main and the variant peaks were pooled separately and further analyzed to identify the molecular structure of the variant peak. Total mass analysis for each peak fraction using ESI-TOF MS shows differences in molecular mass. The fraction of the main peak tends to result in higher molecular masses than the fraction of the variant. The detected masses for the variant are about 600-1000 Da smaller than those for the main peak. Peptide mapping analysis for each peak fraction using Asp-N and Glu-C shows differences in O-glycopeptide profiles at Ser126. The O-glycopeptides were not detected in the fraction of the variant. It is concluded that the variant peak is non-O-glycosylated rHu-EPO and the main peak is fully O-glycosylated rHu-EPO at Ser126.

INTRODUCTION

Human erythropoietin (EPO) is a glycoprotein that stimulates proliferation and differentiation of erythroid precursor cells to more mature erythrocytes (Goldwasser and Kung, 1968). The cloning and expression of the human EPO gene permitted the development of recombinant human EPO (rHu-EPO) as a biopharmaceutical. Since the late 1980s, rHu-EPO has become one of the success stories to emerge from the biotechnology industry (Sytkowski, 2004). The availability of rHu-EPO has provided important new therapeutic options for a variety of dis-

ease and deficiency states (Cazzola et al., 1997; Spivak, 1998).

The rHu-EPO used in pharmaceutical preparations is a 30,400-Dalton, 165-amino-acid glycosylated protein with carbohydrates comprising about 40% of the total molecular weight (Davis et al., 1987). These consist of three N-linked glycans, attached to Asn24, Asn38, and Asn83, and an O-linked glycan, attached to Ser126 (Sasaki et al., 1987; 1988). The carbohydrates of rHu-EPO can vary in their degree of glycosylation and their glycan composition and/or structure due to differences in the mammalian cell lines used to express the protein, differences in the culture conditions, and differences in downstream processing (purification).

The functional roles of carbohydrates for rHu-EPO have been well-documented. In particular, the N-glycosylations are important factors for stability, pharmacokinetics, and biological activity of EPO (Delorme et al., 1992; Toyoda et al., 2000). N-glycans attached to EPO are typically terminated with the negatively charged sugar molecule, sialic acid. The content of sialic acid in rHu-EPO was positively correlated to half-life in the blood and bioactivity (Fukuda et al., 1989; Spivak and Hogans, 1989).

Most studies for glycosylation of EPO have focused on N-glycan structures, whereas little attention has been paid to O-glycosylation. Urinary human EPO and rHu-EPO produced by CHO cell line both have one O-linked glycan, attached to Ser126 which is mostly decorated with a disialylated mucin-type O-glycan (Hokke et al., 1995; Tsuda et al., 1990). The functional roles of O-glycosylation for rHu-EPO are still controversial (Delorme et al., 1992; Wasley et al., 1991). However, sialic acid content from O-glycan of EPO is about 15% of the total and this could contribute to the stability and biological function of EPO, especially to the clearance of EPO from circulation (Castilho et al., 2012; Elliott et al., 2004).

The MALDI-TOF analysis with intact rHu-EPO after removal of N-glycan showed heterogeneity of O-glycan structures according to sialic acid content, where 3 main O-glycoforms were detected, those bearing no sialic acid residue, those with 1 sialic acid residue, and those with 2 sialic acid residues (Llop et al., 2008). In this study, non-O-glycosylated rHu-EPO was detected at a very low level. The analysis of O-glycopeptide level, EPO- α and EPO- β showed different contents of O-glycopeptide from those of NESP (Giménez et al., 2012;

¹Department of Stereoscopic Media, Korean German Institute of Technology, Seoul 157-930, Korea, ²BIONSYSTEMS, Inc., R&D Center, Incheon 406-840, Korea, ³Center for Bioanalysis, Korea Research Institute of Standards and Science, Daejeon 305-340, Korea, ⁴Department of Newmedia, Korean German Institute of Technology, Seoul 157-930, Korea

*Correspondence: jksuh@kgit.ac.kr

Received 18 September, 2014; revised 10 February, 2015; accepted 4 March, 2015; published online 27 May, 2015

Keywords: erythropoietin, O-glycosylation, total mass analysis, Peptide Mapping

Stübiger et al., 2005). Thus, these studies show that variation of O-glycoforms of rHu-EPO are common not only in the same pharmaceutical preparation but also between different pharmaceutical preparations. In this context, the types, structures, and variation of O-glycosylation for rHu-EPO are to be assessed and monitored for therapeutic purpose.

Here we describe a procedure separating non-O-glycosylated rHu-EPO from other glycoforms by RP-HPLC. A UPLC/Q-TOF method was then used to identify and evaluate variation at the O-glycosylation site, Ser126. This study allowed separation and identification of non-O-glycosylated glycoform of rHu-EPO at Ser126.

MATERIALS AND METHODS

Materials

EPO BRP (EDQM, Ph. Eur.) contains a freeze-dried preparation of erythropoietin in vials with a declared content of 250 µg of erythropoietin per vial. This erythropoietin BRP is known as a 50:50 mixture of epoetin alfa (The R.W. Johnson pharmaceutical Research Institute) and epoetin beta (Boehringer-Mannheim, recently Roche).

Trypsin, Asp-N, Glu-C, and PNGaseF were purchased from Roche. Sodium phosphate, monobasic and dibasic, DTT, and guanidine-HCl were purchased from Sigma. Acetonitrile (ACN), trifluoroacetic acid (TFA) and methanol were purchased from B&J. Acetic acid was purchased from J.T. Baker.

RP-HPLC

RP-HPLC analysis was carried out using a Waters Alliance HPLC system equipped with a Waters 2489 UV/Visible detector (Waters, UK). Peak profiling was carried out using a VYDAC214TP54 column (C4, 300A, 5 µm, 4.6 × 250 mm). For quantification, RP-HPLC was performed using the following gradient conditions: solvent A was 0.1% TFA and solvent B was 0.1% TFA, 10% water, and 90% ACN. Protein samples were injected with the volume of 100 µl and a flow rate of 0.5 ml/min. Separation was carried out with the linear gradient of 10-80% B over 25 min. For purity, RP-HPLC was performed using the following gradient conditions: solvent A was 0.15% TFA and solvent B was 0.15% TFA, 10% water, and 90% ACN. Protein samples were injected with the volume of 50 µl and a flow rate of 0.8 ml/min. Separation was performed with the linear gradient of 47-53% B over 25 min.

Total mass analysis

The protein samples were diluted with 20mM sodium phosphate (pH 6.5) at about 1 mg/ml. Mass spectrometry experiments were performed on a Xevo Q-TOF™ system (Waters, UK), equipped with a standard electrospray z-spray source. Each sample was analyzed using a MassPrep Micro Desalting Column (Waters, UK) with UPLC (Waters, UK) and on-line Q-TOF mass spectrometer, Xevo Q-TOF (Waters, UK) at a flow rate of 0.2 ml/min. The capillary voltage was adjusted to 2,700 V, the cone voltage was 40 V, and the source and the desolvation temperature were maintained at 100°C and 200°C, respectively. The instrument was calibrated with NaI before acquisition. The mass spectra obtained in experiments were processed with a Maximum Entropy program (MaxEnt) to deconvolute multiply charged ESI data. The average mass of protein materials was calculated from multiply charged peaks in the Q-TOF™ system. Each multiply charged peak was converted to a mass without positive adducts and then seven converted values were averaged without weighting.

Peptide mapping

The protein sample (100 µg) was reduced and denatured with 1 M DTT and 6 M guanidine-HCl respectively. The denatured protein sample was digested with Asp-N at a ratio of 1 to 20 (Asp-N to protein ratio) for 4 h at 37°C. For Glu-C mapping, Glu-C at a ratio of 1 to 25 was treated for 4 h at 25°C. The obtained peptides were separated using reversed phase (RP) chromatography with an ACQUITY UPLC system (Waters, UK) equipped with an ACQUITY BEH300 C18 column (1.7 µm 2.1 × 150 mm). The 10 µl of peptide solutions were injected on the column with a 0.2 ml/min flow rate at a temperature of 50°C. Mobile phase A was 0.1% TFA in water and B was 0.1% TFA in ACN with the gradient of 3-55% B in 95 min for Asp-N and Glu-C digestions. For trypsin digestion, chromatography was carried out using the method previously described (Song et al., 2014). The peptide map was generated by monitoring the absorbance of the effluent with an UV detector at 215 nm. The assignment of each peptide was based on analysis by on-line electrospray ionization mass spectrometry, Xevo Q-TOF (Waters, UK). MS spectra were obtained with the entire 0.2 ml/min column effluent over the range of 50-3,000 in mass-to-charge ratio with the setting of collision energy at 6 V and cone voltage at 35 V. The peptides were identified using BioPharmaLynx Software (Waters, UK) and the sequences of peptides were determined using PLGS Software (Waters, UK) by searching against theoretical amino acid sequences of EPO.

PNGaseF treatment

The protein sample (100 µg) was reduced and denatured with 1 M DTT and 6 M guanidine-HCl. The denatured protein sample was treated with PNGaseF (1.5 U) for 18 h at 37°C. After inactivating PNGaseF acidity, the deglycosylated protein sample was digested with Asp-N at a ratio of 1 to 20 (Asp-N to protein ratio) for 4 h at 37°C. To identify deglycosylated peptides, the peptides were separated using an RP-UPLC equipped with an ACQUITY BEH300 C18 column (1.7 µm 2.1 × 150 mm). The 10 µl of peptide solutions were injected on the column with a 0.2 ml/min flow rate at a temperature of 50°C. Mobile phase A was 0.1% FA in water and B was 0.1% FA in ACN with the gradient of 3-55% B in 95 min. The peptides were identified using the same methods described in peptide mapping.

MS/MS analysis

MS/MS acquisition was performed using the MS/MS full scan mode, adjusting to encompass the entire charge state of interest. A collision-induced dissociation (CID) at the collision cell was used for fragmentation and 25eV of the collision energy was applied to the collision cell. The sequences of peptides were determined using PLGS Software (Waters, UK) by searching against theoretical amino acid sequences of EPO.

RESULTS

Identification of potential variants of rHu-EPO using RP-HPLC analysis

RP-HPLC analysis for quantification was performed on the Protein C4 column at room temperature using the mobile phases containing 0.1% TFA at a constant flow rate of 0.5 ml/min. The chromatogram for quantification is shown in Fig. 1A and the results are listed in Table 1 which shows apparent purity. Only a single peak was resolved on the chromatogram for quantification, which shows 100% purity of the analyzed rHu-EPO.

Another RP-HPLC method, where samples were resolved by

Table 1. Results of RP-HPLC analysis, quantification and purity methods

Method	Peak label	RT (min)	Peak area	% Area
Quantification	Peak 1	22.11	45206	100
Purity	Peak M	11.14	29236	93.03
	Peak V	13.32	2189	6.97

Peak M represents the main peak fraction from Fig. 1B and Peak V represents the variant peak fraction from Fig. 1B.

Table 2. Molecular masses determined from the fractions of RP-HPLC, the purity method using EI-MS analysis.

Peak label	RT range (min)	Mass range (Da)	Max. intensity at mass (Da)
Peak M	10.0-11.7	28700-31450	30300
Peak V	12.5-14.0	27500-30900	29400

Peak M represents the main peak fraction from Fig. 1B and Peak V represents the variant peak fraction from Fig. 1B.

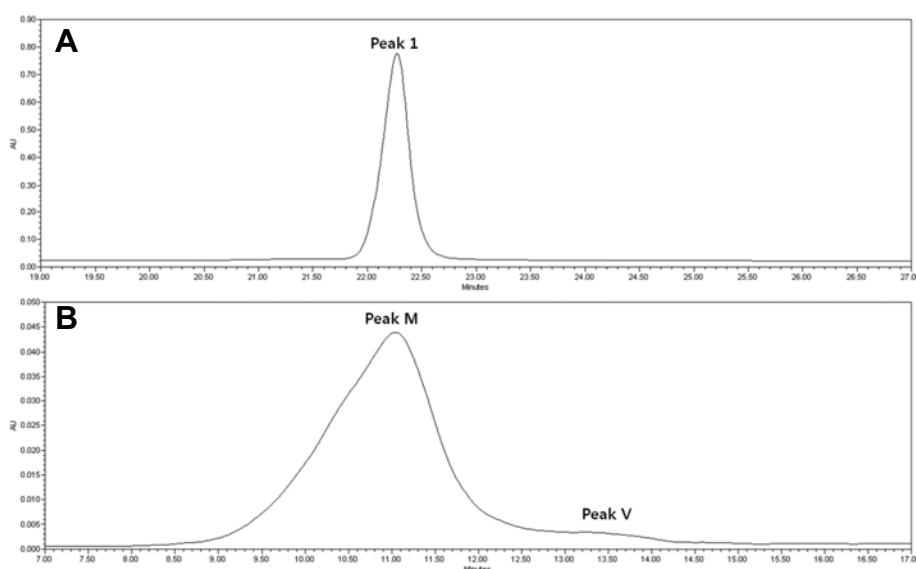


Fig. 1. RP-HPLC analysis of rHu-EPO using a VYDAC214TP54 column (C4, 300A, 5 μ m, 4.6 \times 250 mm). (A) The quantification method was done with the linear gradient of 10-80% B over 25 min (solvent A was 0.1% TFA and solvent B was 0.1% TFA, 10% water, and 90% CAN). (B) The purity method was done with the linear gradient of 47-53% B over 25 min (solvent A was 0.15% TFA and solvent B was 0.15% TFA, 10% water, and 90% ACN).

applying different acetonitrile gradient was performed as a purity method. The purity method applies a HPLC gradient with a significantly lower slope (nearly isocratic conditions, 42-48% ACN). Spreading of the rHu-EPO peaks takes place, so that differences in peak shape and peak-ratios between rHu-EPO batches are observed (Fig. 1B). Obviously spreading of the rHu-EPO peaks (peak broadening) is a consequence of rHu-EPO microheterogeneity (glycosylation pattern). Still, two peaks were nearly baseline separated, one main peak with >90% area and one additional peak with < 10% area) (Table 1).

Identification of rHu-EPO fractions using ESI-MS analysis: molecular mass analysis

Two peaks were separable using the purity method of RP-HPLC. The peaks were labeled Peak M and Peak V respectively (Fig. 1B). Peak M is the main peak eluted with a retention time between 10-12 min and Peak V is the variant peak having a retention time between 12.5-14 min. To identify the structural characteristics of each peak, fractions having corresponding peaks were eluted and collected. The collected fractions were

analyzed using ESI-MS to determine molecular weight for those peaks.

Analysis with ESI-MS gives different results in molecular mass for the collected fractions. The fractions of the main peak (Peak M) tend to result in higher molecular masses than the fractions of the additional peak (Peak V). The determined molecular mass for Peak M was in the range of 28,700-31,450 Da with the maximum intensity on the molecular mass of 30,300 Da (Table 2) and can be assigned to theoretic masses of rHu-EPO showing the theoretical specific oligosaccharide pattern as described in the literature (Council of Europe, 2007).

The determined masses for the variant peak (Peak V) were in the range of 27,500-30,900 Da with the maximum intensity on the molecular mass of 29,400 Da (Table 2). Those values are about 600-1,000 Da smaller than the masses for Peak M but still showing the complex oligosaccharide structure. We assume that these mass differences are most likely due to differences in oligosaccharide structure, especially for O-glycosylation. Further studies by ESI-MS peptide mapping might be able to clearly identify the differences.

Table 3. Results of Identified D16 peptide from rHu-EPO having O-glycosylation on the MS¹ spectrum of Asp-N map

Sequence	Peptide	Modifiers	Calculated mass (Da)	RT (Min)	Determined mass (Da)	Intensity	Mass error (ppm)	% Modified
DAASAA	D16	None	1256.6725	39	1256.6696	33365	-2.3	4.6
PLRTITA	(123-135)	O-G1-2SA	2203.8854	39	2203.9059	360080	9.3	49.5
		O-G1-SA	1912.8450	39	1912.8739	215432	15.1	29.6
		O-GlcNAc-SA	1750.7922	39	1750.8148	60370	12.9	8.3
		O-G1	1621.8046	39	1621.8049	25591	0.2	3.5
		O-GlcNAc	1459.7518	39	1459.7484	33289	-2.3	4.6
AISPPDA	E14	None	1836.9581	44.9	1836.9626	37371	2.4	4.1
ASAAPLR	(118-136)	O-G1-2SA	2784.1709	44.9	2784.202	426760	11.2	46.5
		O-G1-SA	2493.1306	45	2493.1702	270579	15.9	29.5
		O-GlcNAc-SA	2331.0779	44.9	2331.1202	82095	18.1	8.9
		O-GlcNAc	2040.0375	45	2040.0479	52419	5.1	5.7
TITAD		O-G1	2202.0901	45	2202.1042	49353	6.4	5.4

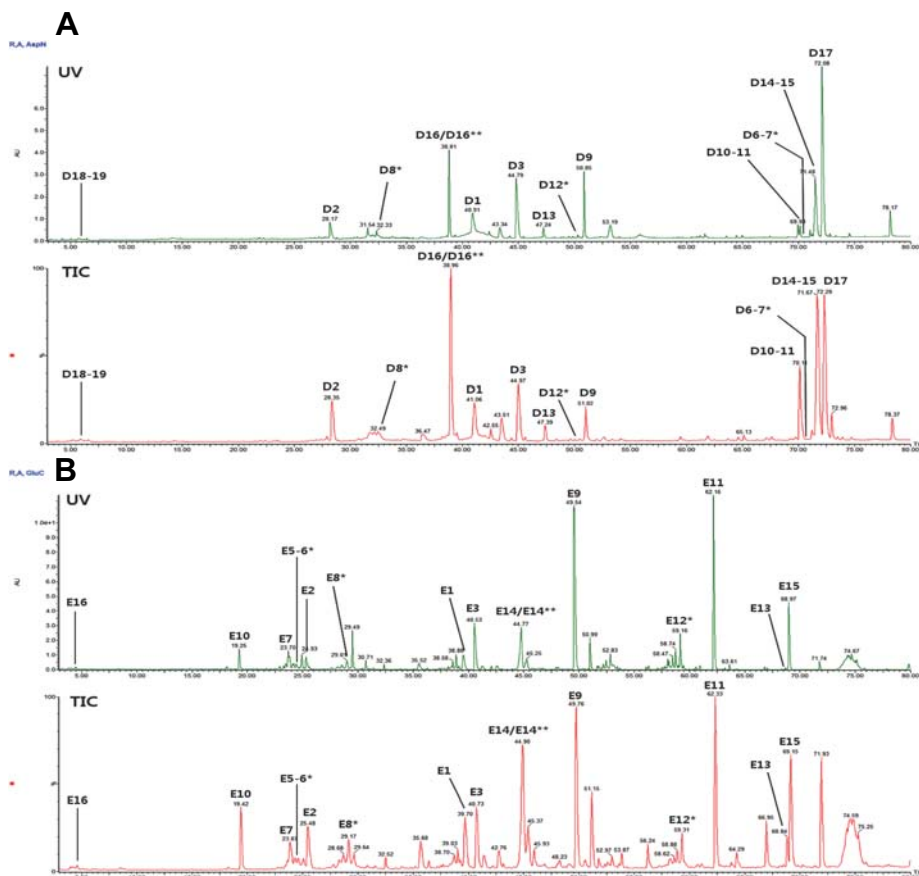


Fig. 2. Asp-N (A) and Glu-C map (B) of rHu-EPO using RP-UPLC equipped with BEH300 C18 column (1.7 μ m 2.1 \times 150 mm) under alkylated and reduced condition. *, N-glycopeptide; **, O-glycopeptide. The assignment of each peptide was done with on-line analysis of Q-TOF mass.

Glycopeptide identification of rHu-EPO using peptide mapping analysis

To clarify the difference of molecular masses between Peak M and Peak V, peptide mapping analysis was carried out using UPLC/ESI-MS. First, a method for peptide mapping for rHu-

EPO was developed for the UPLC with on-line Q-TOF system to check if glycopeptides having O-glycosylation can be detected. Peptide mapping was carried out with endo-protease Asp-N or Glu-C treatment and subsequent separation of peptide fragments by RP-UPLC. The peptide fragments were identified by

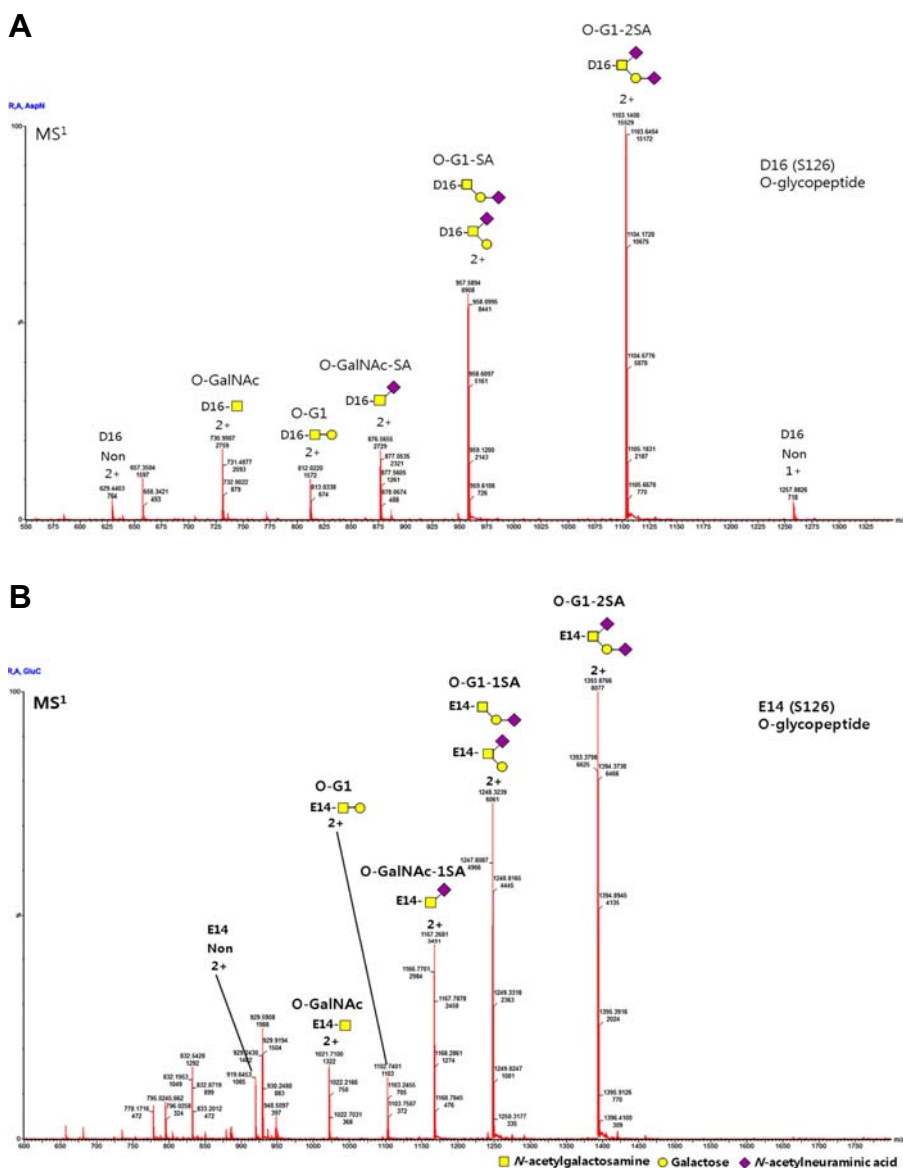


Fig. 3. Identification of D16 peptide of Asp-N map (A) and E14 peptide of Glu-C map (B) from rHu-EPO having O-glycosylation on the MS¹ spectrum. Five structures of O-glycan were identified along with non-glycosylated form. O-GalNAc: GalNAc, O-G1: GalNAc+Gal, O-GalNAc-SA: GalNAc+NeuAc, O-G1-SA: GalNAc+Gal+NeuAc, O-G1-2SA: GalNAc+Gal+2NeuAc.

UV monitoring and on-line Q-TOF mass spectrometry.

rHu-EPO consists of 165 amino acids. 19 peptides are expected with the digestion of Asp-N and 16 peptides are expected with the digestion of Glu-C. D16 and E14 peptides with Ser126 are expected to be glycopeptides with O-glycosylation. A peptide map of rHu-EPO with Asp-N and Glu-C are shown in Fig. 2 along with UV and TIC profile. The Asp-N and Glu-C map covers most amino acid sequences of EPO except small and polar peptides, D5 (¹⁸EAK²⁰) and D6 (²¹EA²²) for Asp-N, or E4 (¹⁹AKE²¹) and E5 (²²AE²³) for Glu-C with the coverage of 97.0% (Supplementary Tables 1 and 2; Supplementary Fig. 1).

Peptides having N-glycosylations were identified on the Asp-N and Glu-C map. To verify the N-glycosylation sites, PNGaseF was treated for deglycosylation and this resulted in conversion of Asn to Asp at the N-glycosylation site. Deglycosylated peptides were identified after digestion of Asp-N endo-protease. Three conversions of Asn to Asp were identified at

the position of Asn24, Asn38, and Asn83 (Supplementary Table 3; Supplementary Figs. 2 and 3). These confirm that N-glycosylations of rHu-EPO were on the Asn24, Asn38, and Asn83.

D16 and E14 peptides having O-glycosylation was identified on a retention time around 39 min for Asp-N and 45 min for Glu-C (Fig. 2). The MS¹ spectrum of D16 and E14 peptides are shown in Fig. 3, which represents the profile of O-glycosylation on D16 and E14 peptides. The majority of O-glycosylation of rHu-EPO was O-G1-2SA [GalNAc(N-acetylgalactosamine)+Gal(Galactose)+2NeuAc(N-acetylneuraminic acid)] which consists of over 45% (Table 3). D16 and E14 peptides without O-glycosylation were also detected on the same fraction of O-glycosylated peptide and the level of D16 and E14 peptides not having O-glycan were about 5% of total intensity for all D16 peptide (Table 3).

We confirmed that the method developed for peptide map-

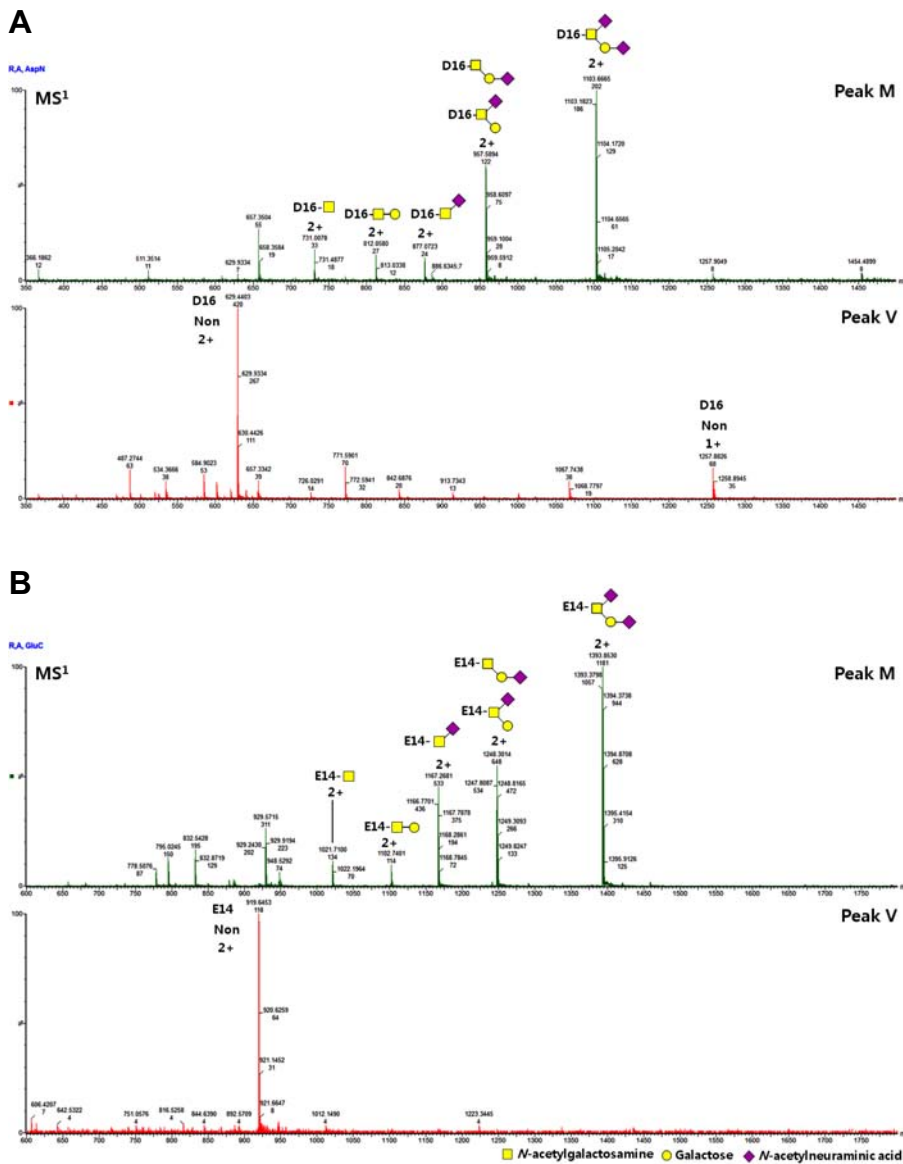


Fig. 4. Identification of D16 peptide of Asp-N map (A) and E14 peptide of Glu-C map (B) on the MS¹ spectrum of peptide map from the fractions of RP-HPLC using the purity method. Peak M represents the main peak fraction from Fig. 1B and Peak V represents the variant peak fraction from Fig. 1B.

ping analysis of rHu-EPO is suitable for identifying D16 and E14 peptides with or without O-glycosylation. This method for peptide mapping was applied to the fractions having corresponding peaks from RP-HPLC analysis to analyze mass difference between two fractions.

Identification of rHu-EPO fractions using peptide mapping analysis

The MS¹ spectra of D16 and E14 peptides from two fractions collected from Peak M and Peak V are shown in Fig. 4. The MS¹ spectrum of the fraction from Peak M shows a similar profile of O-glycosylation from rHu-EPO not fractionated by RP-HPLC except the non-glycosylated D16 and E14 peptide. D16 and E14 peptides without O-glycosylation were also detected but the level of D16 and E14 peptides not having O-glycan was about 10 times lower than that of rHu-EPO not fractionated (Tables 4 and 5). The MS¹ spectrum of the fraction from Peak V shows a totally different profile from that of Peak M. D16 and

E14 peptides having O-glycan were not detected on the MS¹ spectrum from the fraction of Peak V. Only D16 and E14 peptide without O-glycan were detected.

To further characterize the D16 and E14 peptides identified on the MS¹ spectra from the fractions of Peak M and Peak V, the fragmentation spectra of the D16 and E14 peptides with or without O-glycan were analyzed. The D16 and E14 peptide having O-G1-2SA only from the fraction of Peak M was fragmented. The y ions including y₅, y₆, y₇, and y₈ from the D16 peptide were identified and y₁₃^{*} ion having the mass of O-G1-2SA was also identified (Fig. 5 and Supplementary Table 4). Along with y₁₃^{*} having the mass of O-G1-2SA, b₆^{*} ions from D16 peptide having the mass of O-GalNAc (GalNAc), O-G1 (GalNAc+Gal), and G-GalNAc-SA (GalNAc+NeuAc) glycans were also identified (Supplementary Table 4) and this shows that Ser126 is glycosylated.

For further confirmation, the fragmentation spectra of the T13 peptide with or without O-glycan, O-G1-2SA were investigated.

Table 4. Results of identified D16 peptide on the MS¹ spectrum of Asp-N map from the fractions of RP-HPLC using the purity method

Sequence	Peptide	Modifiers	Calculated mass (Da)	RT (Min)	Determined mass (Da)	Intensity	Mass error (ppm)	% Modified
Peak M	D16 (123-135)	None	1256.6725	39	1256.669	1563	-2.5	0.4
		O-G1-2SA	2203.8854	39	2203.911	190080	11.4	49.4
		O-G1-SA	1912.8450	39	1912.874	115583	15.1	30.0
		O-GalNAc-SA	1750.7922	39	1750.801	41849	4.9	10.9
		O-G1	1621.8046	39	1459.762	19320	6.6	5.0
		O-GalNAc	1459.7518	39	1621.801	16271	-2.2	4.2
Peak V	D16 (123-135)	None	1256.6725	39	1256.669	36775	-3.2	100.0
		O-G1-2SA	2203.8854	Not Detected				
		O-G1-SA	1912.8450	Not Detected				
		O-GalNAc-SA	1750.7922	Not Detected				
		O-G1	1621.8046	Not Detected				
		O-GalNAc	1459.7518	Not Detected				

Peak M represents the main peak fraction from Fig. 1B and Peak V represents the variant peak fraction from Fig. 1B.

Table 5. Results of identified E14 peptide on the MS¹ spectrum of Glu-C map from the fractions of RP-HPLC using the purity method

Sequence	Peptide	Modifiers	Calculated mass (Da)	RT (Min)	Determined mass (Da)	Intensity	Mass error (ppm)	% Modified
Peak M	E14 (118-136)	None	1836.9581	45	1836.9607	1929	1.4	1.1
		O-G1-2SA	2784.1709	45	2784.1986	78269	9.9	44.9
		O-G1-SA	2493.1306	45.1	2493.1616	51356	12.4	29.5
		O-GalNAc-SA	2331.0779	45.1	2331.1028	22097	10.7	12.7
		O-G1	2040.0375	45.1	2040.0455	10933	3.9	6.3
		O-GalNAc	2202.0901	45	2202.0991	9715	4.1	5.6
Peak V	E14 (118-136)	None	1256.6725	45	1836.9625	17177	2.4	100.0
		O-G1-2SA	2784.1709	Not Detected				
		O-G1-SA	2493.1306	Not Detected				
		O-GalNAc-SA	2331.0779	Not Detected				
		O-G1	2040.0375	Not Detected				
		O-GalNAc	2202.0901	Not Detected				

Peak M represents the main peak fraction from Fig. 1B and Peak V represents the variant peak fraction from Fig. 1B.

The y ions including y6*, y7*, y8*, y10*, and y11* from the T13 peptide having the mass of O-GalNAc glycan were identified (Supplementary Table 5 and Fig. 6), showing the glycosylation on the Ser126. Thus, combining all of these results, it is concluded that Ser126 is glycosylated.

The D16 peptide without O-glycan only from the fraction of Peak V was fragmented. Several b and y ions were detected. The m/z values of each b and y ion were the same as the expected values. Thus, it is concluded that Ser126 from Peak V is not glycosylated.

DISCUSSION

Separation by RP-HPLC is based on relative differences in the

hydrophobicity of various proteins and their respective interaction (via Van der Waals-type forces) with a hydrocarbon backbone chemically bonded to a silica particle. RP-HPLC may provide a quantification tool and information on molecular variants or degradation products.

We developed two RP-HPLC methods for rHu-EPO, one for quantification and the other for purity analysis. The method for quantification may be capable to quantify rHu-EPO in drug substances as well as in drug products with various formulations. Secondly, the method for purity analysis may be able to monitor process-related variants, which elute in the chromatogram round around 12 min.

Several HPLC methods have been developed for quantification of rHu-EPO (Dudkiewicz-Wilczyńska et al., 2002; Rane et

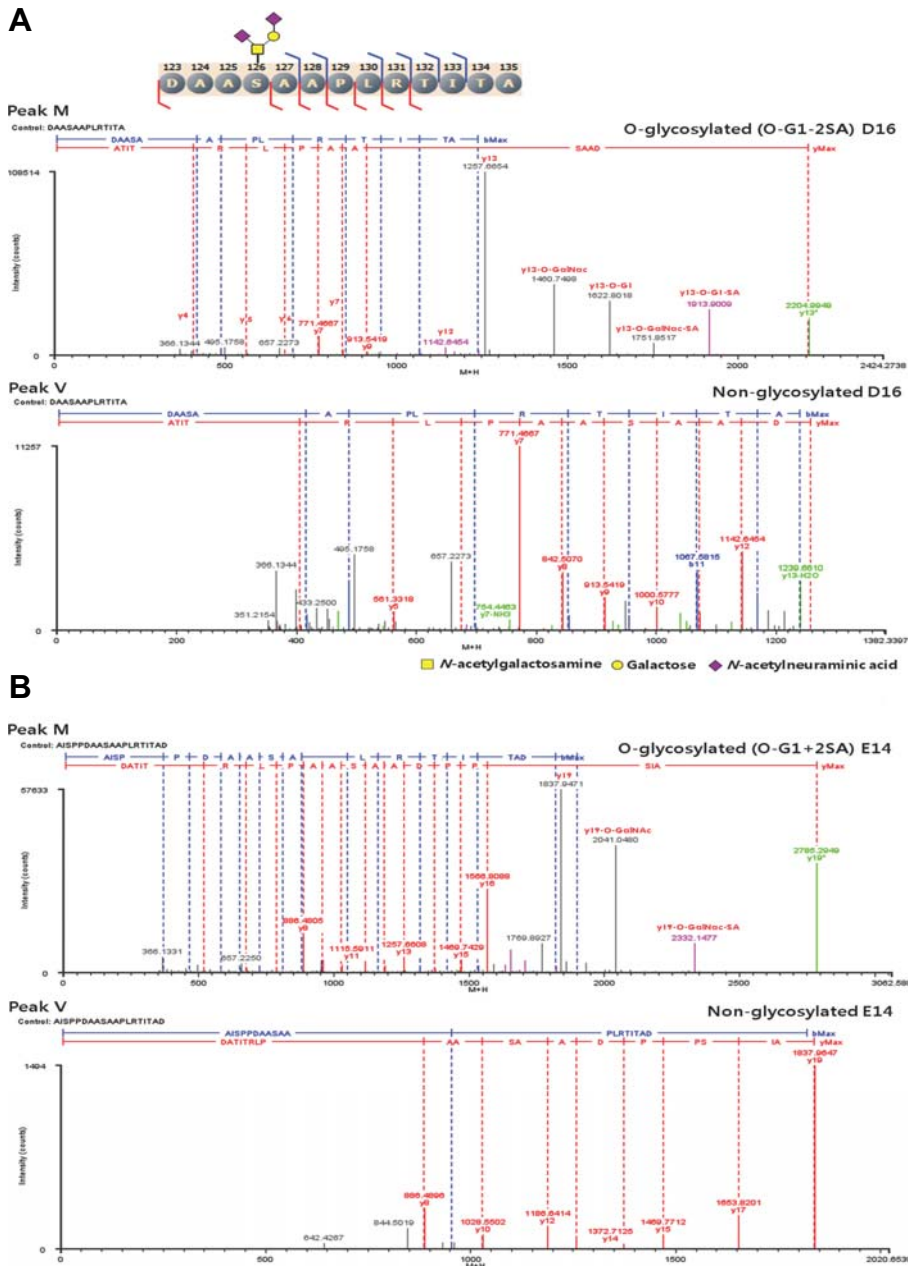


Fig. 5. Fragmentation spectra of D16 peptide of Asp-N map (A) and E14 peptide of Glu-C map (B) from the fractions of RP-HPLC using the purity method. The precursor ion having 1103 m/z of Asp-N map and 1393 m/z of Glu-C map from the fraction of Peak M was fragmented and the structure of O-glycosylation (O-G1-2SA) was confirmed by the product ions. The precursor ion having 629 m/z of Asp-N map and 919 m/z of Glu-C map from the fraction of Peak V was fragmented and the product ions were the same as the expected values which is not modified.

al., 2012; Wilczyńska et al., 2005) with the presence of different stabilizers. Variant peaks were also identified during development but any analytical evidence was not provided for those variants. Thus, our study is the first report with analytical data showing O-glycosylation variants.

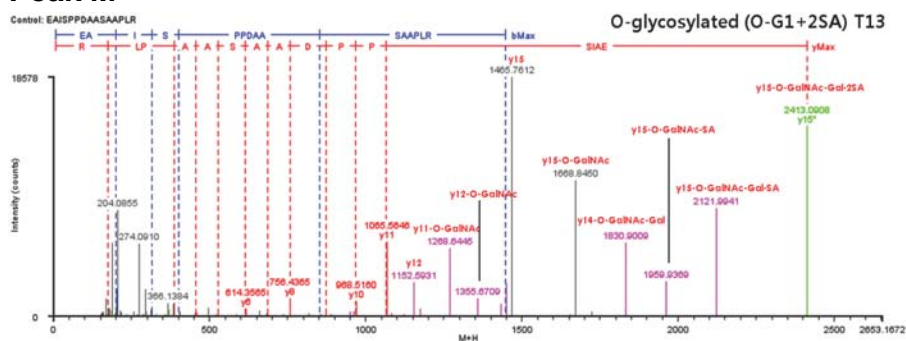
The determined major mass (30,300 Da) for Peak M was similar to the theoretical mass (approximately 30,600 Da) of rHu-EPO as described in the literature (Council of Europe, 2007). These values are about 1,000 Da larger than the major mass (29,400 Da) for Peak V, which suggests for non-O-glycosylation.

We also developed a peptide mapping method for rHu-EPO using UPLC coupled with Q-TOF/MS analysis. Several meth-

ods have been developed for peptide mapping rHu-EPO using HPLC and UPLC with different endo-protease (Gong et al., 2013; Kolarich et al., 2012; Song et al., 2014). This gives high resolution and sensitivity. Using this method, O-glycans with core 1 structure were identified on Ser126 position, which included O-GalNAc, O-G1, O-GalNAc-SA, O-G1-SA (GalNAc+Gal+NeuAc), and O-G1-2SA. The major O-glycan was the disialylated mucin-type O-glycan (O-G1-2SA), which was consistent with previously reported studies (Hokke et al., 1995; Wasley et al., 1991).

Peptide mapping analysis for Peak M gives a similar O-glycan profile to that of rHu-EPO except with a 10-fold lower amount of non-O-glycoylation. However, peptide mapping

Peak M



Peak V

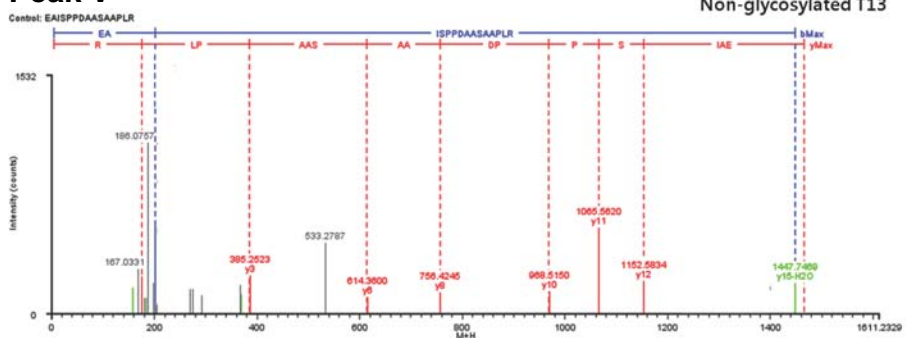


Fig. 6. Fragmentation spectra of T13 peptide of trypsin map from the fractions of RP-HPLC using the purity method. The precursor ion having 1207 m/z from the fraction of Peak M was fragmented and the structure of O-glycosylation (O-G1-2SA) was confirmed by the product ions. The precursor ion having 733 m/z from the fraction of Peak V was fragmented and the product ions were the same as the expected values which is not modified.

analysis for Peak V does not show an O-glycan profile. These results suggest that Peak M contains fully O-glycosylated rHu-EPO and Peak V represents rHu-EPO not glycosylated on S126 for O-glycosylation.

In conclusion, we suggest to apply a quantification method for quantification of rHu- RhEPO and also to monitor process-related impurities. The purity method might be able to monitor rHu-Epo-related degradation on the carbohydrate structure and therefore should be applied as a purity test method. The purity method of RP-HPLC was intended to investigate any chemical substances, which were introduced during the manufacturing processes, and to evaluate non-O-glycosylated rHu-EPO products in the samples.

Note: Supplementary information is available on the Molecules and Cells website (www.molcells.org).

ACKNOWLEDGMENTS

This study was supported partly by a grant from BIONSYTEMS Inc., Seoul, Korea (No.: 2014-A01).

REFERENCES

Castilho, A., Neumann, L., Daskalova, S., Mason, H. S., Steinkellner, H., Altmann, F., and Strasser, R. (2012). Engineering of sialylated mucin-type O-glycosylation in plants. *J. Biol. Chem.* 287, 36518-36526.

Cazzola, M., Mercuriali, F., and Brugnara, C. (1997). Use of recombinant human erythropoietin outside the setting of uremia. *Blood* 89, 4248-4267.

Council of Europe. (2007). *European Pharmacopoeia*, 6th eds. (Strasbourg, France: Council of Europe).

Davis, J.M., Arakawa, T., Strickland, T.W., and Yphantis, D.A. (1987). Characterization of recombinant human erythropoietin produced in Chinese hamster ovary cells. *Biochemistry* 26, 2633-2638.

Delorme, E., Lorenzini, T., Giffin, J., Martin, F., Jacobsen, F., Boone, T., and Elliott, S. (1992). Role of glycosylation on the secretion and biological activity of erythropoietin. *Biochemistry* 31, 9871-9876.

Dudkiewicz-Wilczyńska, J., Snyckerski, A., and Tautt, J. (2002). Application of high-performance size exclusion chromatography to the determination of erythropoietin in pharmaceutical preparations. *Acta pol. Pharm.* 59, 83-86.

Elliott, S., Egrie, J., Browne, J., Lorenzini, T., Busse, L., Rogers, N., and Ponting, I. (2004). Control of rHuEPO biological activity: the role of carbohydrate. *Exp. Hematol.* 32, 1146-1155.

Fukuda, M.N., Sasaki, H., Lopez, L., and Fukuda, M. (1989). Survival of recombinant erythropoietin in the circulation: the role of carbohydrates. *Blood* 73, 84-89.

Giménez, E., Ramos-Hernan, R., Benavente, F., Barbosa, J., and Sanz-Nebot, V. (2012). Analysis of recombinant human erythropoietin glycopeptides by capillary electrophoresis electrospray-time of flight-mass spectrometry. *Anal. Chim. acta* 709, 81-90.

Goldwasser, E., and Kung, C.K. (1968). Progress in the purification of erythropoietin. *Ann. N Y Acad. Sci.* 149, 49-53.

Gong, B., Burnina, I., Stadheim, T.A., and Li, H. (2013). Glycosylation characterization of recombinant human erythropoietin produced in glycoengineered *Pichia pastoris* by mass spectrometry. *J. Mass Spectrom.* 48, 1308-1317.

Hokke, C.H., Bergwerff, A.A., Dedem, G.W., Kamerling, J.P., and Vliegthart, J.F. (1995). Structural analysis of the sialylated N- and O-linked carbohydrate chains of recombinant human erythropoietin expressed in chinese hamster ovary cells. *Eur. J. Biochem.* 228, 981-1008.

Kolarich, D., Jensen, P.H., Altmann, F., and Packer, N.H. (2012). Determination of site-specific glycan heterogeneity on glycoproteins. *Nat. Protoc.* 7, 1285-1298.

Llop, E., Gutiérrez-Gallego, R., Segura, J., Mallorquí, J., and Pascual, J.A. (2008). Structural analysis of the glycosylation of gene-activated erythropoietin (epoetin delta, Dynepo). *Anal. Biochem.* 383, 243-254.

Rane, S.S., Ajameri, A., Mody, R., and Padmaja, P. (2012). Development and validation of RP-HPLC and RP-UPLC methods for quantification of erythropoietin formulated with human serum albumin. *J. Pharm. Anal.* 2, 160-165.

- Sasaki, H., Bothner, B., Dell, A., and Fukuda, M. (1987). Carbohydrate structure of erythropoietin expressed in Chinese hamster ovary cells by a human erythropoietin cDNA. *J. Biol. Chem.* 262, 12059-12076.
- Sasaki, H., Ochi, N., Dell, A., and Fukuda, M. (1988). Site-specific glycosylation of human recombinant erythropoietin: analysis of glycopeptides or peptides at each glycosylation site by fast atom bombardment-mass spectrometry. *Biochemistry* 27, 8618-8626.
- Song, K.E., Byeon, J., Moon, D.B., Kim, H.H., Choi, Y.J., and Suh, J.K. (2014) Structural identification of modified amino acids on the interface between EPO and its receptor from EPO BRP, human recombinant erythropoietin by LC/MS analysis. *Mol. Cells* 37, 819-826.
- Spivak, J.L. (1998). The biology and clinical applications of recombinant erythropoietin. *Semin. Oncol.* 25, 7-11.
- Spivak, J.L., and Hogans, B.B. (1989). The *in vivo* metabolism of recombinant human erythropoietin in the rat. *Blood* 73, 90-99.
- Stübiger, G., Marchetti, M., Nagano, M., Grimm, R., Gmeiner, G., Reichel, C., and Allmaier, G. (2005). Characterization of N- and O-glycopeptides of recombinant human erythropoietins as potential biomarkers for doping analysis by means of microscale sample purification combined with MALDI-TOF and quadrupole IT/RTOF mass spectrometry. *J. Cell. Sci.* 28, 1764-1778.
- Sytkowski A.J. (2004). Erythropoietin: blood, brain and beyond (Weinheim, Germany: Wiley-VCH Verlag).
- Toyoda, T., Itai, T., Arakawa, T., Aoki, K.H., and Yamaguchi, H. (2000). Stabilization of human recombinant erythropoietin through interactions with the highly branched N-glycans. *J. Biochem.* 128, 731-737.
- Tsuda, E., Kawanishi, G., Ueda, M., Masuda, S., and Sasaki, R. (1990). The role of carbohydrate in recombinant human erythropoietin. *Eur. J. Biochem.* 188, 405-411.
- Wasley, L.C., Timony, G., Murtha, P., Stoudemire, J., Dornier, A.J., Caro, J., Krieger, M., and Kaufman, R.J. (1991). The importance of N- and O-linked oligosaccharides for the biosynthesis and *in vitro* and *in vivo* biologic activities of erythropoietin. *Blood* 77, 2624-2632.
- Wilczyńska, J.D., Roman, I., and Anuszevska, E. (2005). The separation of EPO from other proteins in medical products formulated with different stabilizers. *Acta Pol. Pharm.* 62, 177-182.